

Charged Fusion Product Detector Study
Florida International University
Department of Physics

Author:
Carlos LOPEZ

Supervisor:
Dr. Werner BOEGLIN

Abstract: The results of experiments performed by a member of the Florida International University's experimental plasma physics research group will be presented. The work was done in preparation for the testing of a proton detection system implemented at the Mega Amp Spherical Tokamak at the Culham Centre for Fusion Energy in Oxfordshire, England. Monte Carlo methods were implemented in Python to model and calculate the solid angle of acceptance of the detectors. The results of the computer simulation were compared with results of a spectroscopy experiment using an alpha particle emitter. This experiment was implemented in order to measure the counting rate of the detector, where particular interest was given to the change in said counting rate as the source position changed. The results of both works will be compared and presented.

October 11, 2013

Background

Plasma is the fourth fundamental state of matter, it is a quasi-neutral gaseous mixture comprised of positively charged ions and negatively charged electrons. As a consequence; plasmas can be manipulated, shaped, and confined if the appropriate configurations of external electromagnetic fields are applied to them. [4] The tokamak device was invented for this purpose. The standard configuration uses horizontally and vertically aligned magnetic fields to warp its plasma into a donut-like shape, forcing the nuclei and electrons to travel in helically shaped trajectories.

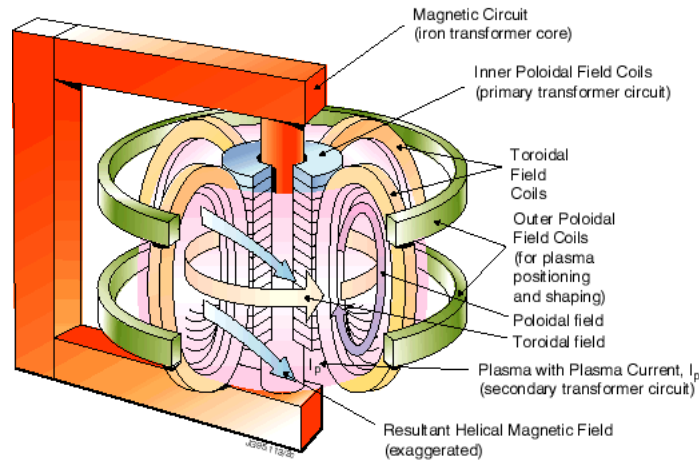
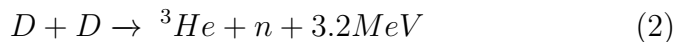


Figure 1: Tokamak Field Configuration [1]

The plasma can then be heated by running the appropriate current through the transformer coil, forcing a secondary current to run through the gas itself. Following this is the neutral beam injection, which involves firing a stream of neutral atoms towards the center of the tokamak. As these atoms hit the plasma, they become ion-

ized and transfer energy into the gas great enough to allow fusion reactions to occur.

Nuclear fusion is the reaction that takes place when two light atomic nuclei combine to form a new and heavier type of atomic nucleus. The tokamak's job is to force the nuclei to overcome the repulsive Coulomb barrier and allow for the attractive nuclear potential to meld them together. These reactions give off a relatively clean source of energy that is hoped to be harvested for the purposes of commercial electricity production. The reactions of interest involve the fusion of hydrogen-2, or the deuteron (D),



where T is triton (or hydrogen-3), p is the proton, n is the neutron, and 3He is helium-3. [4] To study instabilities within the tokamak plasma, the trajectories of the protons are analyzed using a sophisticated detection system at the facilities involving the Mega Amp Spherical Tokamak (MAST) at the Culham Centre for Fusion Energy in Oxfordshire, England. To aid in this project, a computational and experimental study of the counting efficiency of the detection instruments was undertaken at the nuclear physics laboratory at Florida International University in Miami, Florida.

Introduction

A silicon surface barrier detector is a semiconductor diode that has a very thin window on its face which allows charged particles to enter it. Applying voltage across this device means that the electric field will sweep out charged particles out of an area on the detector's face called the depletion region. When charged particles enter the detector, most of their energy is deposited into the depletion region, with the ensuing separation of positive and negative carriers creating a potential difference that is proportional to the energy of the incident radiation. [7]

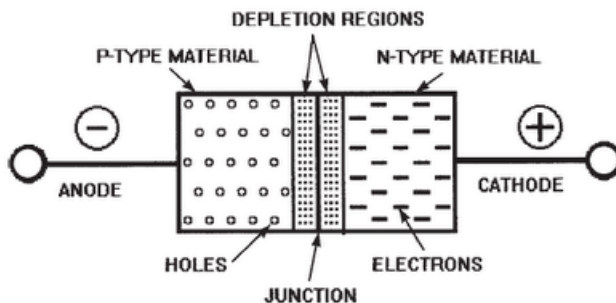


Figure 2: Diode Depletion Layer [6]

The efficiency and solid angle of acceptance are properties of the detector that warrant study. The efficiency of a detector relates the number of pulses outputted by the detector to the number of particles incident on it. It is of convenience to quantify the detector's efficiency and subdivide them into two classes, absolute (aka geometric) and intrinsic, they are defined as such:

$$\epsilon_{abs} = \frac{\textit{number of pulses recorded}}{\textit{number of particles emitted by source}} \quad (3)$$

$$\epsilon_{int} = \frac{\textit{number of pulses recorded}}{\textit{number of particles incident on detector}} \quad (4)$$

For the purposes of this study, the intrinsic efficiency is assumed to be 100 percent, and so it is left to the task of calculating the geometrical efficiency in terms of the solid angle of the acceptance cone of the detector.

The solid angle is generally defined by the integral over the detector surface area that faces a source, and in units of steradians is of the form:

$$\Omega = \int \frac{dA \cos \theta}{R^2} \quad (5)$$

where R represents the relative position vector between the source and a surface element dA , and θ is the angle between the normal to the surface element and the source direction. [7] It is of interest to derive the solid angle for the particular cases of a point source located along and off of the axis of a right circular cylinder.

For the first case:

$$\begin{aligned}
\Omega &= \int \frac{dA \cos \theta}{R^2} \\
&= \int r dr d\phi \frac{h}{\sqrt{r^2 + h^2}} \frac{1}{r^2 + h^2} \\
&= \int \frac{hr dr d\phi}{\sqrt{r^2 + h^2}} \\
&= h2\pi \int \frac{r dr}{\sqrt{r^2 + h^2}} \\
&= h2\pi \frac{1}{h} \left(1 - \frac{h}{\sqrt{r^2 + h^2}}\right) \\
&= 2\pi \left(1 - \frac{h}{\sqrt{r^2 + h^2}}\right) \tag{6}
\end{aligned}$$

Taking the Taylor expansion of the second equation inside the parentheses is needed to complete the proof. Recall that the general form of the Taylor series for a function $f(x)$ at $x = a$ up to the second derivative is the following [3]

$$f(x) = f(a) + f'(a)(x - a) + f''(a) \frac{(x - a)^2}{2!} \tag{7}$$

Some manipulation must be done to fit the function in question

$$\frac{d}{\sqrt{d^2 + a^2}} = \frac{d}{d\sqrt{1 + \frac{a^2}{d^2}}} = \frac{1}{\sqrt{1 + \frac{a^2}{d^2}}} = \frac{1}{\sqrt{1 + x^2}} \tag{8}$$

Therefore yielding the following useful result

$$\begin{aligned}
f(x) &= \frac{1}{\sqrt{1+a^2}} - \frac{a}{\sqrt[3]{1+a^2}}(x-a) \\
&\quad + (1-2a^2)\sqrt{1+a^2}\frac{(x-a)^2}{2}\Big|_{a=0} \\
&= 1 - \frac{x^2}{2}
\end{aligned} \tag{9}$$

Finally recalling the fact that $x = (a/d)$ and returning to equation (6), the value for the solid angle on the axis of the right circular cylinder is computed

$$\begin{aligned}
\Omega &= 2\pi\left(1 - \left(1 - \frac{x^2}{2}\right)\right) \\
&= 2\pi\left(1 - 1 + \frac{a^2}{d^2}\right) \\
&= \pi\frac{a^2}{d^2}
\end{aligned} \tag{10}$$

For the off-axis case of a source located some distance $(x,0,0)$ away from the origin yields the following relative position vector, recalling the position vector is offset due to its projections in x and y planes at the azimuthal angle ϕ

$$\vec{R} = (x + r \cos \phi)\hat{x} + (r \sin \phi)\hat{y} + h\hat{z} \tag{11}$$

Plugging this back into equation (5) yields the following result:

$$\Omega = \int \frac{hrdrd\phi}{\sqrt[3]{(x + r \cos \phi)^2 + (r \sin \phi)^2 + h^2}} \quad (12)$$

This is an integral that cannot be solved analytically, however the numerical techniques of the Monte Carlo method allows one to bypass that stage all together and perform an even more direct calculation.

Monte Carlo Simulation

Monte Carlo is a method of computing values such as probabilities by means of a large number of repeated random samples and obtaining a numerical result. This is performed using a program written in Python, simulating the decay of a radiation source as it emits particles uniformly in all directions. The code will see what fraction of those particles enter into the detector and tabulate values for the geometrical efficiency.

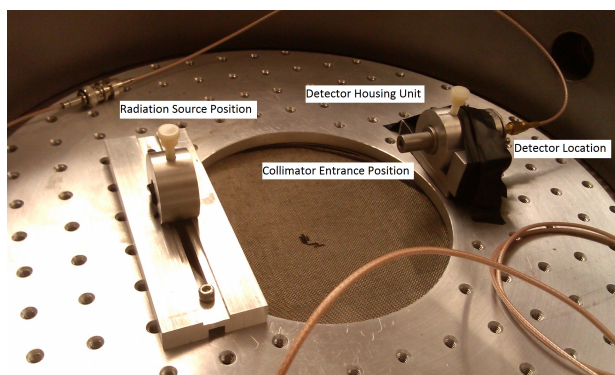


Figure 3: Vacuum Chamber

The radiation source position is the origin, the collimator entrance is 154mm away in the z-direction, and the detector is 204mm away also in the z-direction. The collimator is used to screen out only those particles which fall into a very specific angle so as to mimic collections of protons in the tokamak. The code will then count as a 'hit' those particles that have touched the circular face of the detector only after having hit the appropriate part of the collimator's plane as well.

As was shown in preceding sections, the solid angle is calculated from the values of the polar and azimuthal angles, and the monte carlo algorithm randomly samples these angles in a uniform fashion. The former of which is defined according to the geometry. The position of the source is the origin, (0,0,0). The position of the collimator-detector housing is in the z-direction, with the collimator entrance at $z_c=(0,0,154)$ mm and the detector face is at $z_d=(0,0,204)$ mm, with a radius of $rc = 2.5$ mm. The radiation will actually go forth beyond the plane of the detector, so an offset of 20mm is included in the calculation of θ in the following manner

$$\theta_{min} = \arctan\left(\frac{2 * rc + offset}{z_d}\right) \quad (13)$$

The cosine of the polar angle and the azimuthal angle are sampled randomly in the following ranges

$$\cos \theta_{min} \leq \cos \theta \leq 1$$

$$0 \leq \phi \leq 2\pi$$

Therefore the unit vector in the direction of the propagation in of the radiation in spherical coordinates can be calculated

$$\vec{u} = \sin \theta \cos \phi \hat{x} + \sin \theta \sin \phi \hat{y} + \cos \theta \hat{z} \quad (14)$$

The position of the source is variable, so the general position vector is given by the equation

$$\vec{R} = \vec{s} + t\vec{u} \quad (15)$$

To find the unknown x and y coordinates of \vec{R} , take the known z coordinate, solve for the line parameter t and then calculate the final values of x and y:

$$t = \frac{z}{\cos \theta} \implies x = x_s + tu_x, y = y_s + tu_y \quad (16)$$

The issue at hand is to confirm if the above values fall into the collimator entrance and then check if those values will also fall into the face of the detector, this is done simply by checking those values against the following inequality

$$x^2 + y^2 < R^2 \quad (17)$$

The ratio of the number of x and y coordinates that satisfy equation (17) versus the total number of coordinates checked against it are used to calculate the solid angle according to the following relationship

$$\Omega = \frac{N_{in}}{N} \Delta(\cos \theta) \Delta(\phi) = \frac{N_{in}}{N} 2\pi(1 - \cos \theta_{min}) \quad (18)$$

Graphs pertaining to the distance of the source from the detector were created, highlighting the difference in size between the projection of the radiation hitting the plane of the detector versus those particles that actually hit the detector itself.

The following images highlight an idealized picture of the radiation being emitted from the source.

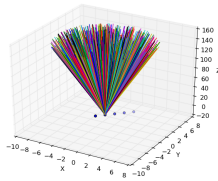


Figure 4: Emission 1

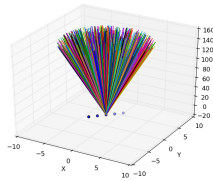


Figure 5: Emission 2

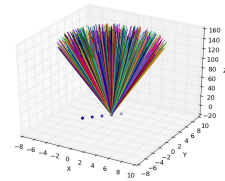


Figure 6: Emission 3

These images highlight the radiation as it hits the plane of the detector, with those that manage to make it into the detector highlighted in red.

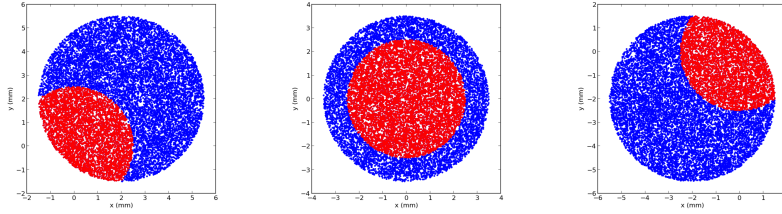
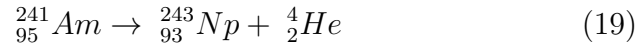


Figure 7: Projection 1 **Figure 8:** Projection 2 **Figure 9:** Projection 3

Alpha Particle Spectroscopy

The experimental portion of the project involved the use of a 241-Americium source undergoing to following nuclear decay scheme:



where ${}_{95}^{241}\text{Am}$ is Americium-241, ${}_{93}^{243}\text{Np}$ is Neptunium-243, and ${}_2^4\text{He}$ is the alpha particle. [8] It contains two protons and two neutrons and its detection serves as the means of physically testing the counting efficiency of the detector. The series of steps involved in the experiment are organized into the following flow chart

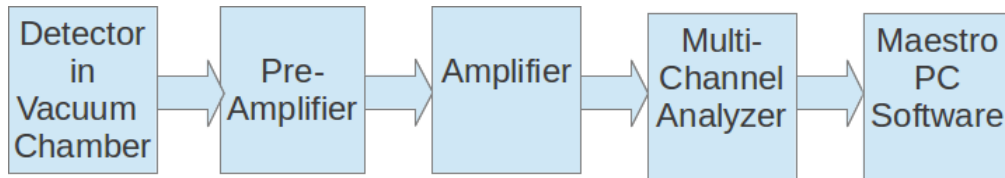


Figure 10: Experimental Procedure

Alpha particles carry energies of between 4-8 MeV and their travel can be stopped by an ordinary piece of paper, and will not travel more than 3.6cm in air. [7] For this reason, a vacuum chamber

in conjunction with a Varian SD-450 vacuum pump is implemented to bring down the atmosphere in the chamber to as low as 200mTorr (263×10^{-6} atmospheric pressure). The implemented preamplifier is the model 2003BT from the Canberra Corporation and the implemented amplifier is the model 570 from ORTEC. The multi-channel analyzer is the Easy-MCA from ORTEC connected to the Maestro-32 software for Windows.

Spectroscopy details measuring the energy of particles emitted by radiation sources, where the emission is produced by various nuclear reaction such as in equation (19). An energy spectrum is a function giving the distribution of particles in terms of their energy. For the purposes of this experiment, the integral energy spectrum will be focused on, which is defined as the number of particles with energy greater than or equal to some energy E . It can be defined analytically as:

$$N(E) = \int n(E)dE \quad (20)$$

where $n(E)dE$ is the number of particles with energies between E and $E+dE$, and $n(E)$ alone is the number of particles per unit energy interval. [8] Consider a typical spectrum produced by the source, which was collected via the Maestro software and then highlighted and analyzed using Python:

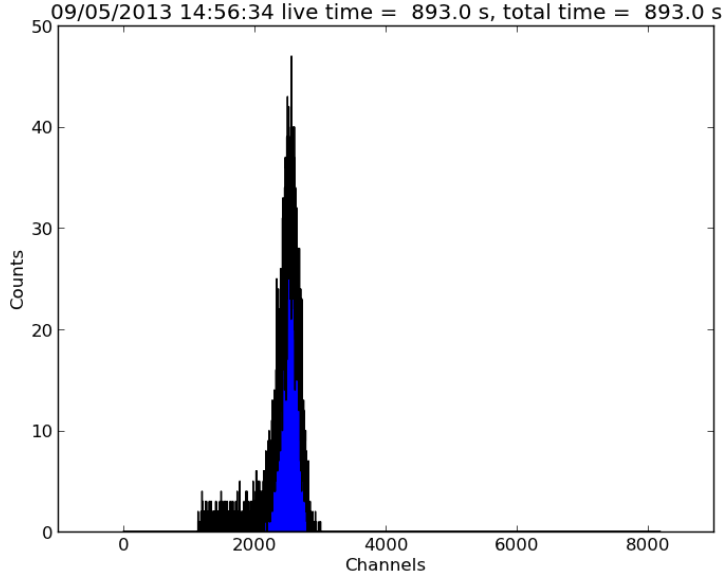


Figure 11: Alpha Peak

The one pronounced peak in the spectrum demonstrates the mono-energetic nature of the source, emitting particles with an unknown energy E_o , it implies that the value of $n(E)$ approaches zero for any energies other than $E = E_o$. The integral spectrum $N(E)$ is almost constant for all energies $E \leq E_o$, since only those particles with energy E_o exist. [8] It is not possible to calculate a numeric value for the E_o of this source, since it is impossible to calibrate the equipment for a source of energy that is not previously known.

From the values observed, the activity of the radiation source can be calculated from the following relationship

$$Activity = \left(\frac{\Sigma_{\alpha}}{t_L}\right)\left(\frac{4\pi s^2}{\pi r^2}\right) \quad (21)$$

where Σ_α is the gross number of counts underneath the peak, t_L is the live time of the measurement in seconds, s is the distance from the source to the detector in cm, and r is the detector radius also in cm. [5] According to equation (21), the value of the activity is proportional to a scaled solid angle by the count rate, for the ideal case of the source looking at the detector straight on the value is $6 \times 10^{-6} Ci$.

Results

The solid angle is a function of the geometry, and changes according to the distance the source is from the detector, therefore the solid angle from the simulations and count rate from the experiments have been graphs separately. The uncertainties in the data are calculated according to the following equation, which in its general form assumes there exists some function u dependent on the variables x , y , and z . The uncertainty in u is then

$$\sigma_u = \sqrt{\left(\frac{\partial u}{\partial x} \sigma_x\right)^2 + \left(\frac{\partial u}{\partial y} \sigma_y\right)^2 + \left(\frac{\partial u}{\partial z} \sigma_z\right)^2} \quad (22)$$

where for example $\partial u / \partial x$ is the rate of change of u with respect to x and σ_x is the standard deviation of u also with respect to x . [2]

Therefore, according to equation (22), the uncertainty in the solid angle is

$$\sigma_\Omega = \frac{\sqrt{N_{in}}}{N} 2\pi(1 - \cos \theta_{min}) \quad (23)$$

The uncertainty in the count rate, also according to equation (22), is

$$\sigma_r = \sqrt{\frac{\sum \alpha}{t_L^2}} \quad (24)$$

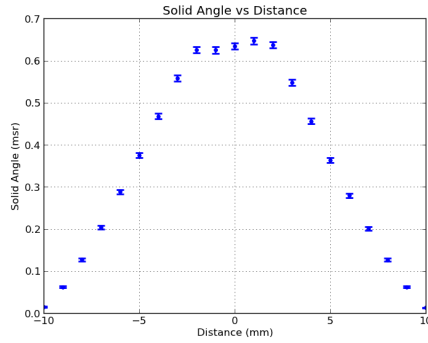


Figure 12: Computational Data

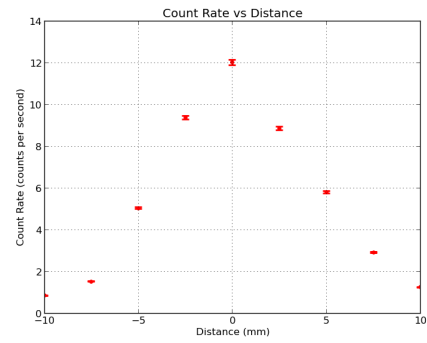


Figure 13: Experimental Data

To obtain a measure of how the two data sets correlate with each other, both data sets and their uncertainty measurements have been normalized to unit-less quantities and plotted on top of each other as functions of the distance, and the output of this is presented below

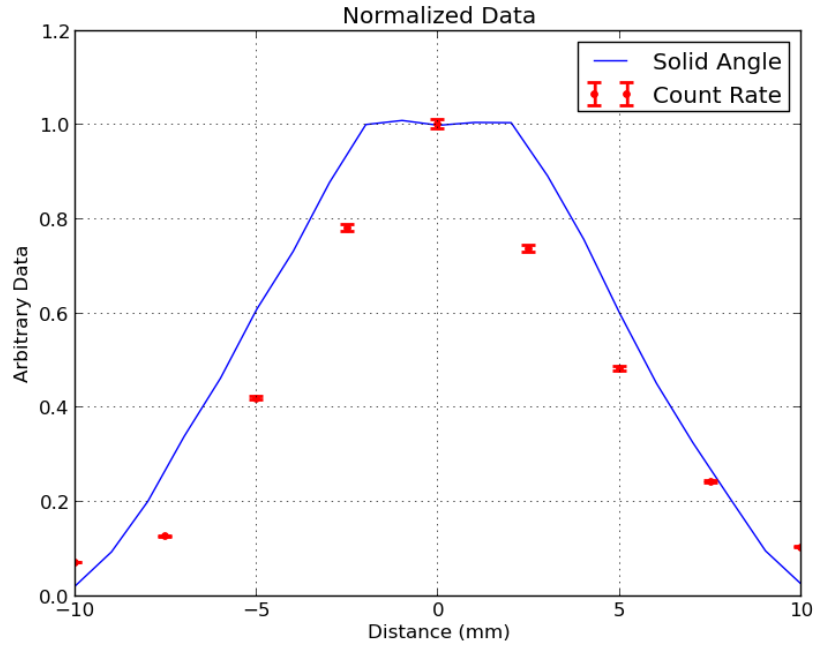


Figure 14: Activity as a function of distance

Conclusions and Future Work

A functional relationship between the solid angle of acceptance of the detector and its distance from the radiation source was studied, with the experimental results serving to validate the computational simulations and vice versa. Issues have arisen in the analysis that involve disconnects between the shapes of the computational and experimental data sets. Specifically the saturation that is observed in the computational data set is not observed in the more peak like nature of the experimental data. The cause of this deviation is at the present time unknown, though several explanations are plau-

sible. These would involve inefficiencies in the numerical method used to compute the data or the measurements of the distances involved in the experiment were not measured to within the appropriate degree of accuracy. To correct for this, several things need to be re-examined. More efficient computational methods need to be explored and more accurate measurements need to be made with regard to the experimental setup. A greater number of measurements need to be taken during future experiments so as to improve the statistics and calculate the true collection efficiency of the detectors. This is crucial for the comparison and analysis of the data from the tokamak diagnostic.

Acknowledgements

I should like to thank my family and friends for all of their love and support. I would like to thank my advisors Dr. Werner Boeglin and Phd Candidate Mrs. Ramona Perez for their unwaivering patience, unbridled support, and superb guidance of me throughout the goings on of this project. I would like to thank the McNair scholars program for allowing me this wonderful opportunity to improve my skills as a scientist and to broaden my horizons as a human being.

References

- [1] European Fusion Development Agreement. Jet operation at high current. www.efda.org/jet.
- [2] Phillip Bevington and Keith Robinson. *Data Reduction and Error Analysis for the Physical Sciences*. Mc-Graw Hill, New York, New York, 2002.
- [3] Mary Boas. *Mathematical Methods in the Physical Sciences*. Wiley, New York, New York, 2005.
- [4] Francis F. Chen. *Introduction to Plasma Physics and Controlled Fusion*. Springer, New York, New York, 2006.
- [5] Jeromey Duggan and The Ortec Corporation. Alpha particle spectroscopy with silicon charged particle detectors. *AN34 Experiments in Nuclear Science*, 2010.
- [6] Electronics Hub. P-n junction diode characteristics and working. www.electronicshub.org.
- [7] Glenn F. Knoll. *Radiation Detection and Measurement*. John-Wiley and Sons Inc, Hoboken, New Jersey, 1989.
- [8] Nicholas Tsoulfanidis. *Measurement and Detection of Radiation*. Hemisphere Publishing Corporation, New York, New York, 1983.